
UCB Exploration via Q -Ensembles

Richard Y. Chen
OpenAI
richardchen@openai.com

Szymon Sidor
OpenAI
szymon@openai.com

Pieter Abbeel
OpenAI
University of California, Berkeley
pabbeel@cs.berkeley.edu

John Schulman
OpenAI
joschu@openai.com

Abstract

We show how an ensemble of Q^* -functions can be leveraged for more effective exploration in deep reinforcement learning. We build on well established algorithms from the bandit setting, and adapt them to the Q -learning setting. We propose an exploration strategy based on upper-confidence bounds (UCB). Our experiments show significant gains on the Atari benchmark.

1 Introduction

Deep reinforcement learning seeks to learn mappings from high-dimensional observations to actions. Deep Q -learning (Mnih et al. [14]) is a leading technique that has been used successfully, especially for video game benchmarks. However, fundamental challenges remain, for example, improving sample efficiency and ensuring convergence to high quality solutions. Provably optimal solutions exist in the bandit setting and for small MDPs, and at the core of these solutions are exploration schemes. However these provably optimal exploration techniques do not extend to deep RL in a straightforward way.

Bootstrapped DQN (Osband et al. [18]) is a previous attempt at adapting a theoretically verified approach to deep RL. In particular, it draws inspiration from *posterior sampling for reinforcement learning* (PSRL, Osband et al. [16], Osband and Van Roy [15]), which has near-optimal regret bounds. PSRL samples an MDP from its posterior each episode and exactly solves Q^* , its optimal Q -function. However, in high-dimensional settings, both approximating the posterior over MDPs and solving the sampled MDP are intractable. Bootstrapped DQN avoids having to establish and sample from the posterior over MDPs by instead approximating the posterior over Q^* . In addition, bootstrapped DQN uses a multi-headed neural network to represent the Q -ensemble. While the authors proposed bootstrapping to estimate the posterior distribution, their empirical findings show best performance is attained by simply relying on different initializations for the different heads, not requiring the sampling-with-replacement process that is prescribed by bootstrapping.

In this paper, we design new algorithms that build on the Q -ensemble approach from Osband et al. [18]. However, instead of using posterior sampling for exploration, we use the uncertainty estimates from the Q -ensemble. Specifically, we propose the UCB exploration strategy. This strategy is inspired by established UCB algorithms in the bandit setting and constructs uncertainty estimates of the Q -values. In this strategy, agents are optimistic and take actions with the highest UCB. We demonstrate that our algorithms significantly improve performance on the Atari benchmark.

2 Background

2.1 Notation

We model reinforcement learning as a Markov decision process (MDP). We define an MDP as $(\mathcal{S}, \mathcal{A}, T, R, p_0, \gamma)$, in which both the state space \mathcal{S} and action space \mathcal{A} are discrete, $T : \mathcal{S} \times \mathcal{A} \times \mathcal{S} \mapsto \mathbb{R}_+$ is the transition distribution, $R : \mathcal{S} \times \mathcal{A} \mapsto \mathbb{R}$ is the reward function, and $\gamma \in (0, 1]$ is a discount factor, and p_0 is the initial state distribution. We denote a transition experience as $\tau = (s, a, r, s')$ where $s' \sim T(s'|s, a)$ and $r = R(s, a)$. A policy $\pi : \mathcal{S} \mapsto \mathcal{A}$ specifies the action taken after observing a state. We denote the Q -function for policy π as $Q^\pi(s, a) := \mathbb{E}_\pi [\sum_{t=0}^{\infty} \gamma^t r_t | s_0 = s, a_0 = a]$. The optimal Q^* -function corresponds to taking the optimal policy

$$Q^*(s, a) := \sup_{\pi} Q^\pi(s, a)$$

and satisfies the Bellman equation

$$Q^*(s, a) = \mathbb{E}_{s' \sim T(\cdot|s, a)} [r + \gamma \cdot \max_{a'} Q^*(s', a')].$$

2.2 Exploration in reinforcement learning

A notable early optimality result in reinforcement learning was the proof by Watkins and Dayan [27, 26] that an online Q -learning algorithm is guaranteed to converge to the optimal policy, provided that every state is visited an infinite number of times. However, the convergence of Watkins' Q -learning can be prohibitively slow in MDPs where ϵ -greedy action selection explores state space randomly. Later work developed reinforcement learning algorithms with provably fast (polynomial-time) convergence (Kearns and Singh [11], Brafman and Tennenholtz [5], Strehl et al. [21]). At the core of these provably-optimal learning methods is some exploration strategy, which actively encourages the agent to visit novel state-action pairs. For example, R-MAX optimistically assumes that infrequently-visited states provide maximal reward, and delayed Q -learning initializes the Q -function with high values to ensure that each state-action is chosen enough times to drive the value down.

Since the theoretically sound RL algorithms are not computationally practical in the deep RL setting, deep RL implementations often use simple exploration methods such as ϵ -greedy and Boltzmann exploration, which are often sample-inefficient and fail to find good policies. One common approach of exploration in deep RL is to construct an exploration bonus, which adds a reward for visiting state-action pairs that are deemed to be novel or informative. In particular, several prior methods define an exploration bonus based on a density model or dynamics model. Examples include VIME by Houthoofd et al. [10], which uses variational inference on the forward-dynamics model, and Tang et al. [24], Bellemare et al. [3], Ostrovski et al. [19], Fu et al. [9]. While these methods yield successful exploration in some problems, a major drawback is that this exploration bonus does not depend on the rewards, so the exploration may focus on irrelevant aspects of the environment, which are unrelated to reward.

2.3 Bayesian reinforcement learning

Earlier works on Bayesian reinforcement learning include Dearden et al. [7, 8]. Dearden et al. [7] studied Bayesian Q -learning in the model-free setting and learned the distribution of Q^* -values through Bayesian updates. The prior and posterior specification relied on several simplifying assumptions, some of which are not compatible with the MDP setting. Dearden et al. [8] took a model-based approach that updates the posterior distribution of the MDP. The algorithm samples from the MDP posterior multiple times and solving the Q^* values at every step. This approach is only feasible for RL problems with very small state space and action space. Strens [22] proposed posterior sampling for reinforcement learning (PSRL). PSRL instead takes a single sample of the MDP from the posterior in each episode and solves the Q^* values. Recent works including Osband et al. [16] and Osband and Van Roy [15] established near-optimal Bayesian regret bounds for episodic RL. Sorg et al. [20] models the environment and constructs exploration bonus from variance of model parameters. These methods are experimented on low dimensional problems only, because the computational cost of these methods is intractable for high dimensional RL.

2.4 Bootstrapped DQN

Inspired by PSRL, but wanting to reduce computational cost, prior work developed approximate methods. Osband et al. [17] proposed randomized least-square value iteration for linearly-parameterized value functions. Bootstrapped DQN Osband et al. [18] applies to Q -functions parameterized by deep neural networks. Bootstrapped DQN (Osband et al. [18]) maintains a Q -ensemble, represented by a multi-head neural net structure to parameterize $K \in \mathbb{N}_+$ Q -functions. This multi-head structure shares the convolution layers but includes multiple “heads”, each of which defines a Q -function Q_k .

Bootstrapped DQN diversifies the Q -ensemble through two mechanisms. The first mechanism is independent initialization. The second mechanism applies different samples to train each Q -function. These Q -functions can be trained simultaneously by combining their loss functions with the help of a random mask $m_\tau \in \mathbb{R}_+^K$

$$L = \sum_{\tau \in B_{\text{mini}}} \sum_{k=1}^K m_\tau^k \cdot (Q^k(s, a; \theta) - y_\tau^{Q^k})^2,$$

where $y_\tau^{Q^k}$ is the target of the k th Q -function. Thus, the transition τ updates Q_k only if m_τ^k is nonzero. To avoid the overestimation issue in DQN, bootstrapped DQN calculates the target value $y_\tau^{Q^k}$ using the approach of Double DQN (Van Hasselt et al. [25]), such that the current $Q_k(\cdot; \theta_t)$ network determines the optimal action and the target network $Q_k(\cdot; \theta^-)$ estimates the value

$$y_\tau^{Q^k} = r + \gamma \max_a Q^k(s', \arg\max_a Q_k(s', a; \theta_t); \theta^-).$$

In their experiments on Atari games, Osband et al. [18] set the mask $m_\tau = (1, \dots, 1)$ such that all $\{Q_k\}$ are trained with the same samples and their only difference is initialization. Bootstrapped DQN picks one Q_k uniformly at random at the start of an episode and follows the greedy action $a_t = \arg\max_a Q_k(s_t, a)$ for the whole episode.

3 Approximating Bayesian Q -learning with Q -Ensembles

Ignoring computational costs, the ideal Bayesian approach to reinforcement learning is to maintain a posterior over the MDP. However, with limited computation and model capacity, it is more tractable to maintain a posterior of the Q^* -function. In this section, we first derive a posterior update formula for the Q^* -function under full exploration assumption and this formula turns out to depend on the transition Markov chain (Section 3.1). The Bellman equation emerges as an approximation of the log-likelihood. This motivates using a Q -ensemble as a particle-based approach to approximate the posterior over Q^* -function and an Ensemble Voting algorithm (Section 3.2).

3.1 Bayesian update for Q^*

An MDP is specified by the transition probability T and the reward function R . Unlike prior works outlined in Section 2.3 which learned the posterior of the MDP, we will consider the joint distribution over (Q^*, T) . Note that R can be recovered from Q^* given T . So (Q^*, T) determines a unique MDP. In this section, we assume that the agent samples (s, a) according to a fixed distribution. The corresponding reward r and next state s' given by the MDP append to (s, a) to form a transition $\tau = (s, a, r, s')$, for updating the posterior of (Q^*, T) . Recall that the Q^* -function satisfies the Bellman equation

$$Q(s, a) = r + \mathbb{E}_{s' \sim T(\cdot|s, a)} \left[\gamma \max_{a'} Q(s', a') \right].$$

Denote the joint prior distribution as $p(Q^*, T)$ and the posterior as \tilde{p} . We apply Bayes’ formula to expand the posterior:

$$\begin{aligned} \tilde{p}(Q^*, T|\tau) &= \frac{p(\tau|Q^*, T) \cdot p(Q^*, T)}{Z(\tau)} \\ &= \frac{p(Q^*, T) \cdot p(s'|Q^*, T, (s, a)) \cdot p(r|Q^*, T, (s, a, s')) \cdot p(s, a)}{Z(\tau)}, \end{aligned} \quad (1)$$

where $Z(\tau)$ is a normalizing constant and the second equality is because s and a are sampled randomly from \mathcal{S} and \mathcal{A} . Next, we calculate the two conditional probabilities in (1). First,

$$p(s'|Q^*, T, (s, a)) = p(s'|T, (s, a)) = T(s'|s, a), \quad (2)$$

where the first equality is because given T , Q^* does not influence the transition. Second,

$$\begin{aligned} p(r|Q^*, T, (s, a, s')) &= p(r|Q^*, T, (s, a)) \\ &= \mathbb{1}_{\{Q^*(s, a) = r + \gamma \cdot \mathbb{E}_{s'' \sim T(\cdot|s, a)} \max_{a'} Q^*(s'', a')\}} \\ &:= \mathbb{1}(Q^*, T), \end{aligned} \quad (3)$$

where $\mathbb{1}_{\{\cdot\}}$ is the indicator function and in the last equation we abbreviate it as $\mathbb{1}(Q^*, T)$. Substituting (2) and (3) into (1), we obtain the joint posterior of Q^* and T after observing an additional randomly sampled transition τ

$$\tilde{p}(Q^*, T|\tau) = \frac{p(Q^*, T) \cdot T(s'|s, a) \cdot p(s, a)}{Z(\tau)} \cdot \mathbb{1}(Q^*, T). \quad (4)$$

We point out that the exact Q^* -posterior update (4) is intractable in high-dimensional RL due to the large space of (Q^*, T) .

3.2 Q -learning with Q -ensembles

In this section, we make several approximations to the Q^* -posterior update and derive a tractable algorithm. First, we approximate the prior of Q^* by sampling $K \in \mathbb{N}_+$ independently initialized Q^* -functions $\{Q_k\}_{k=1}^K$. Next, we update them as more transitions are sampled. The resulting $\{Q_k\}$ approximate samples drawn from the posterior. The agent chooses the action by taking a majority vote from the actions determined by each Q_k . We display our method, Ensemble Voting, in Algorithm 1.

We derive the update rule for $\{Q_k\}$ after observing a new transition $\tau = (s, a, r, s')$. At iteration i , given $Q^* = Q_{k,i}$ the joint probability of (Q^*, T) factors into

$$p(Q_{k,i}, T) = p(Q^*, T|Q^* = Q_{k,i}) = p(T|Q_{k,i}). \quad (5)$$

Substitute (5) into (4) and we obtain the corresponding posterior for each $Q_{k,i+1}$ at iteration $i+1$ as

$$\tilde{p}(Q_{k,i+1}, T|\tau) = \frac{p(T|Q_{k,i}) \cdot T(s'|s, a) \cdot p(s, a)}{Z(\tau)} \cdot \mathbb{1}(Q_{k,i+1}, T). \quad (6)$$

$$\tilde{p}(Q_{k,i+1}|\tau) = \int_T \tilde{p}(Q_{k,i+1}, T|\tau) dT = p(s, a) \cdot \int_T \tilde{p}(T|Q_{k,i}, \tau) \cdot \mathbb{1}(Q_{k,i+1}, T) dT. \quad (7)$$

We update $Q_{k,i}$ to $Q_{k,i+1}$ according to

$$Q_{k,i+1} \leftarrow \operatorname{argmax}_{Q_{k,i+1}} \tilde{p}(Q_{k,i+1}|\tau). \quad (8)$$

We first derive a lower bound of the the posterior $\tilde{p}(Q_{k,i+1}|\tau)$:

$$\begin{aligned} \tilde{p}(Q_{k,i+1}|\tau) &= p(s, a) \cdot \mathbb{E}_{T \sim \tilde{p}(T|Q_{k,i}, \tau)} \mathbb{1}(Q_{k,i+1}, T) \\ &= p(s, a) \cdot \mathbb{E}_{T \sim \tilde{p}(T|Q_{k,i}, \tau)} \lim_{c \rightarrow +\infty} \exp(-c[Q_{k,i+1}(s, a) - r - \gamma \mathbb{E}_{s'' \sim T(\cdot|s, a)} \max_{a'} Q_{k,i+1}(s'', a')]^2) \\ &= p(s, a) \cdot \lim_{c \rightarrow +\infty} \mathbb{E}_{T \sim \tilde{p}(T|Q_{k,i}, \tau)} \exp(-c[Q_{k,i+1}(s, a) - r - \gamma \mathbb{E}_{s'' \sim T(\cdot|s, a)} \max_{a'} Q_{k,i+1}(s'', a')]^2) \\ &\geq p(s, a) \cdot \lim_{c \rightarrow +\infty} \exp(-c \mathbb{E}_{T \sim \tilde{p}(T|Q_{k,i}, \tau)} [Q_{k,i+1}(s, a) - r - \gamma \mathbb{E}_{s'' \sim T(\cdot|s, a)} \max_{a'} Q_{k,i+1}(s'', a')]^2) \\ &= p(s, a) \cdot \mathbb{1}_{\mathbb{E}_{T \sim \tilde{p}(T|Q_{k,i}, \tau)} [Q_{k,i+1}(s, a) - r - \gamma \mathbb{E}_{s'' \sim T(\cdot|s, a)} \max_{a'} Q_{k,i+1}(s'', a')]^2 = 0}. \end{aligned} \quad (9)$$

where we apply a limit representation of the indicator function in the third equation. The fourth equation is due to the bounded convergence theorem. The inequality is Jensen's inequality. The last equation (9) replaces the limit with an indicator function.

A sufficient condition for (8) is to maximize the lower-bound of the posterior distribution in (9) by ensuring the indicator function in (9) to hold. We can replace (8) with the following update

$$Q_{k,i+1} \leftarrow \operatorname{argmin}_{Q_{k,i+1}} \mathbb{E}_{T \sim \tilde{p}(T|Q_{k,i}, \tau)} [Q_{k,i+1}(s, a) - (r + \gamma \cdot \mathbb{E}_{s'' \sim T(\cdot|s, a)} \max_{a'} Q_{k,i+1}(s'', a'))]^2. \quad (10)$$

However, (10) is not tractable because the expectation in (10) is taken with respect to the posterior $\tilde{p}(T|Q_{k,i}, \tau)$ of the transition T . To overcome this challenge, we approximate the posterior update by reusing the one-sample next state s' from τ such that

$$Q_{k,i+1} \leftarrow \underset{Q_{k,i+1}}{\operatorname{argmin}} [Q_{k,i+1}(s, a) - (r + \gamma \cdot \max_{a'} Q_{k,i+1}(s', a'))]^2. \quad (11)$$

Instead of updating the posterior after each transition, we use an experience replay buffer B to store observed transitions and sample a minibatch B_{mini} of transitions (s, a, r, s') for each update. In this case, the batched update of each $Q_{k,i}$ to $Q_{k,i+1}$ becomes a standard Bellman update

$$Q_{k,i+1} \leftarrow \underset{Q_{k,i+1}}{\operatorname{argmin}} \mathbb{E}_{(s,a,r,s') \in B_{\text{mini}}} [Q_{k,i+1}(s, a) - (r + \gamma \cdot \max_{a'} Q_{k,i+1}(s', a'))]^2. \quad (12)$$

For stability, Algorithm 1 also uses a target network for each Q_k as in Double DQN in the batched update. We point out that the action choice of Algorithm 1 is exploitation only. In the next section, we propose two exploration strategies.

Algorithm 1 Ensemble Voting

- 1: **Input:** $K \in \mathbb{N}_+$ copies of independently initialized Q^* -functions $\{Q_k\}_{k=1}^K$.
 - 2: Let B be a replay buffer storing transitions for training
 - 3: **for** each episode **do**
 - 4: Obtain initial state from environment s_0
 - 5: **for** step $t = 1, \dots$ until end of episode **do**
 - 6: Pick an action according to $a_t = \text{MajorityVote}(\{\operatorname{argmax}_a Q_k(s_t, a)\}_{k=1}^K)$
 - 7: Execute a_t . Receive state s_{t+1} and reward r_t from the environment
 - 8: Add (s_t, a_t, r_t, s_{t+1}) to replay buffer B
 - 9: At learning interval, sample random minibatch and update $\{Q_k\}$
 - 10: **end for**
 - 11: **end for**
-

4 UCB Exploration Strategy Using Q -Ensembles

In this section, we propose optimism-based exploration by adapting the UCB algorithms (Auer et al. [2], Audibert et al. [1]) from the bandit setting. The UCB algorithms maintain an upper-confidence bound for each arm, such that the expected reward from pulling each arm is smaller than this bound with high probability. At every time step, the agent optimistically chooses the arm with the highest UCB. Auer et al. [2] constructed the UCB based on empirical reward and the number of times each arm is chosen. Audibert et al. [1] incorporated the empirical variance of each arm’s reward into the UCB, such that at time step t , an arm A_t is pulled according to

$$A_t = \operatorname{argmax}_i \left\{ \hat{r}_{i,t} + c_1 \cdot \sqrt{\frac{\hat{V}_{i,t} \log(t)}{n_{i,t}}} + c_2 \cdot \frac{\log(t)}{n_{i,t}} \right\}$$

where $\hat{r}_{i,t}$ and $\hat{V}_{i,t}$ are the empirical reward and variance of arm i at time t , $n_{i,t}$ is the number of times arm i has been pulled up to time t , and c_1, c_2 are positive constants.

We extend the intuition of UCB algorithms to the RL setting. Using the outputs of the $\{Q_k\}$ functions, we construct a UCB by adding the empirical standard deviation $\tilde{\sigma}(s_t, a)$ of $\{Q_k(s_t, a)\}_{k=1}^K$ to the empirical mean $\tilde{\mu}(s_t, a)$ of $\{Q_k(s_t, a)\}_{k=1}^K$. The agent chooses the action that maximizes this UCB

$$a_t \in \operatorname{argmax}_a \left\{ \tilde{\mu}(s_t, a) + \lambda \cdot \tilde{\sigma}(s_t, a) \right\}, \quad (13)$$

where $\lambda \in \mathbb{R}_+$ is a hyperparameter.

We present Algorithm 2, which incorporates the UCB exploration. The hyperparameter λ controls the degrees of exploration. In Section 5, we compare the performance of our algorithms on Atari games using a consistent set of parameters.

Algorithm 2 UCB Exploration with Q -Ensembles

```
1: Input: Value function networks  $Q$  with  $K$  outputs  $\{Q_k\}_{k=1}^K$ . Hyperparameter  $\lambda$ .
2: Let  $B$  be a replay buffer storing experience for training.
3: for each episode do
4:   Obtain initial state from environment  $s_0$ 
5:   for step  $t = 1, \dots$  until end of episode do
6:     Pick an action according to  $a_t \in \operatorname{argmax}_a \{\tilde{\mu}(s_t, a) + \lambda \cdot \tilde{\sigma}(s_t, a)\}$ 
7:     Receive state  $s_{t+1}$  and reward  $r_t$  from environment, having taken action  $a_t$ 
8:     Add  $(s_t, a_t, r_t, s_{t+1})$  to replay buffer  $B$ 
9:     At learning interval, sample random minibatch and update  $\{Q_k\}$  according to (12)
10:  end for
11: end for
```

5 Experiment

In this section, we conduct experiments to answer the following questions:

1. does Ensemble Voting, Algorithm 1, improve upon existing algorithms including Double DQN and bootstrapped DQN?
2. is the proposed UCB exploration strategy of Algorithm 2 effective in improving learning compared to Algorithm 1?
3. how does UCB exploration compare with prior exploration methods such as the count-based exploration method of Bellemare et al. [3]?

We evaluate the algorithms on each Atari game of the Arcade Learning Environment (Bellemare et al. [4]). We use the multi-head neural net architecture of Osband et al. [18]. We fix the common hyperparameters of all algorithms based on a well-tuned double DQN implementation, which uses the Adam optimizer (Kingma and Ba [12]), different learning rate and exploration schedules compared to Mnih et al. [14]. Appendix A tabulates the hyperparameters. The number of $\{Q_k\}$ functions is $K = 10$. Experiments are conducted on the OpenAI Gym platform (Brockman et al. [6]) and trained with 40 million frames and 2 trials on each game.

We take the following directions to evaluate the performance of our algorithms:

1. we compare Algorithm 1 against Double DQN and bootstrapped DQN,
2. we isolate the impact of UCB exploration by comparing Algorithm 2 with $\lambda = 0.1$, denoted as `ucb exploration`, against Algorithm 1.
3. we compare Algorithm 1 and Algorithm 2 with the count-based exploration method of Bellemare et al. [3].
4. we aggregate the comparison according to different categories of games, to understand when our methods are superior.

Figure 1 compares the normalized learning curves of all algorithms across Atari games. Overall, Ensemble Voting, Algorithm 1, outperforms both Double DQN and bootstrapped DQN. With exploration, `ucb exploration` improves further by outperforming Ensemble Voting.

In Appendix B, we tabulate detailed results that compare our algorithms, Ensemble Voting and `ucb exploration`, against prior methods. In Table 2, we tabulate the maximal mean reward in 100 consecutive episodes for Ensemble Voting, `ucb exploration`, bootstrapped DQN and Double DQN. Without exploration, Ensemble Voting already achieves higher maximal mean reward than both Double DQN and bootstrapped DQN in a majority of Atari games. `ucb exploration` achieves the highest maximal mean reward among these four algorithms in 30 games out of the total 49 games evaluated. Figure 2 displays the learning curves of these five algorithms on a set of six Atari games. Ensemble Voting outperforms Double DQN and bootstrapped DQN. `ucb exploration` outperforms Ensemble Voting.

In Table 3, we compare our proposed methods with the count-based exploration method A3C+ of Bellemare et al. [3] based on their published results of A3C+ trained with 200 million frames. We

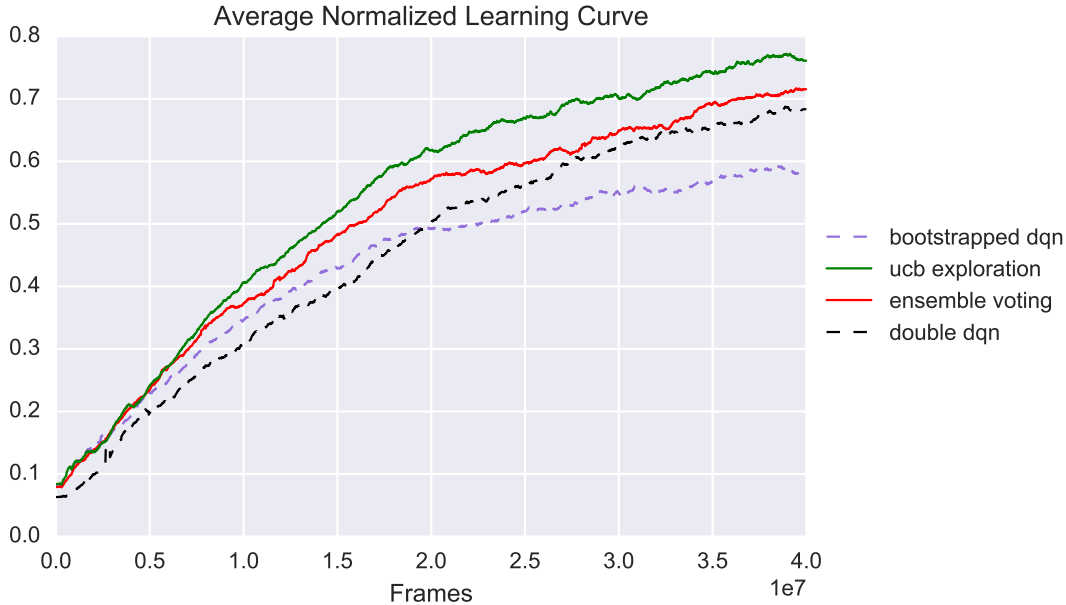


Figure 1: Comparison of algorithms in normalized learning curve. The normalized learning curve is calculated as follows: first, we normalize learning curves for all algorithms in the same game to the interval $[0, 1]$; next, average the normalized learning curve from all games for each algorithm.

point out that even though our methods were trained with only 40 million frames, much less than A3C+’s 200 million frames, UCB exploration achieves the highest average reward in 28 games, Ensemble Voting in 10 games, and A3C+ in 10 games. Our approach outperforms A3C+.

Finally to understand why and when the proposed methods are superior, we aggregate the comparison results according to four categories: Human Optimal, Score Explicit, Dense Reward, and Sparse Reward. These categories follow the taxonomy in Table 1 of Ostrovski et al. [19]. Out of all games evaluated, 23 games are Human Optimal, 8 are Score Explicit, 8 are Dense Reward, and 5 are Sparse Reward. The comparison results are tabulated in Table 4, where we see ucb exploration achieves top performance in more games than Ensemble Voting, Double DQN, and Bootstrapped DQN in the categories of Human Optimal, Score Explicit, and Dense Reward. In Sparse Reward, both ucb exploration and Ensemble Voting achieve best performance in 2 games out of total of 5. Thus, we conclude that ucb exploration improves prior methods consistently across different game categories within the Arcade Learning Environment.

6 Conclusion

We proposed a Q -ensemble approach to deep Q -learning, a computationally practical algorithm inspired by Bayesian reinforcement learning that outperforms Double DQN and bootstrapped DQN, as evaluated on Atari. The key ingredient is the UCB exploration strategy, inspired by bandit algorithms. Our experiments show that the exploration strategy achieves improved learning performance on the majority of Atari games.

References

- [1] Jean-Yves Audibert, Rémi Munos, and Csaba Szepesvári. Exploration–exploitation tradeoff using variance estimates in multi-armed bandits. *Theor. Comput. Sci.*, 410(19):1876–1902, 2009.
- [2] Peter Auer, Nicolo Cesa-Bianchi, and Paul Fischer. Finite-time analysis of the multiarmed bandit problem. *Mach. Learn.*, 47(2-3):235–256, 2002.

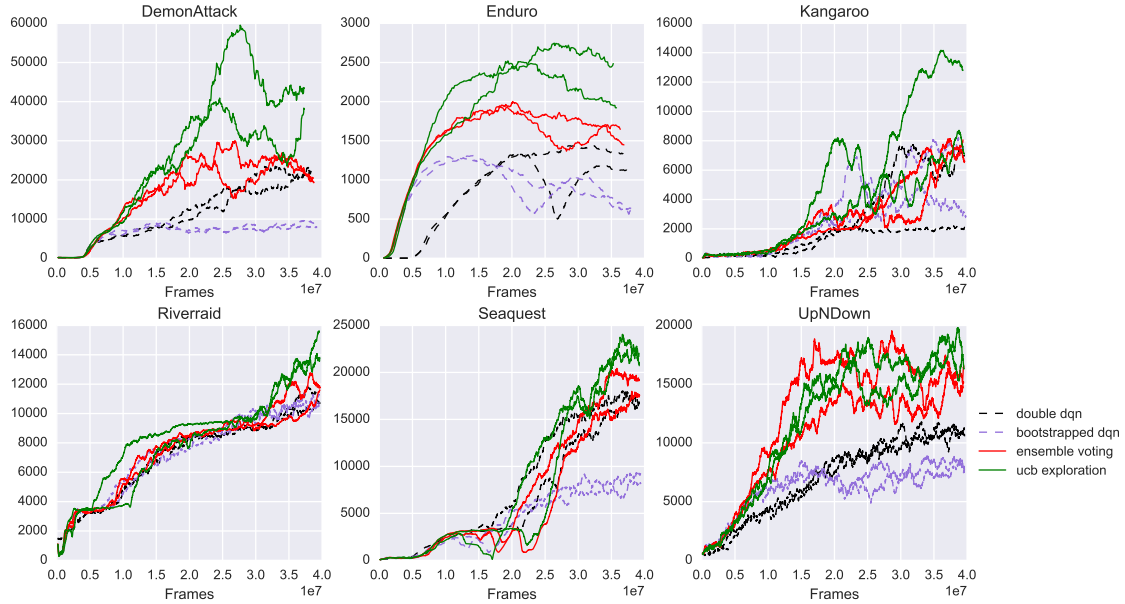


Figure 2: Comparison of UCB Exploration and Ensemble Voting against Double DQN and Bootstrapped DQN.

- [3] Marc Bellemare, Sriram Srinivasan, Georg Ostrovski, Tom Schaul, David Saxton, and Remi Munos. Unifying count-based exploration and intrinsic motivation. In *NIPS*, pages 1471–1479, 2016.
- [4] Marc G Bellemare, Yavar Naddaf, Joel Veness, and Michael Bowling. The arcade learning environment: An evaluation platform for general agents. *J. Artif. Intell. Res.*, 47:253–279, 2013.
- [5] Ronen I Brafman and Moshe Tennenholtz. R-max-a general polynomial time algorithm for near-optimal reinforcement learning. *J. Mach. Learn. Res.*, 3(Oct):213–231, 2002.
- [6] Greg Brockman, Vicki Cheung, Ludwig Pettersson, Jonas Schneider, John Schulman, Jie Tang, and Wojciech Zaremba. OpenAI Gym. *arXiv preprint arXiv:1606.01540*, 2016.
- [7] Richard Dearden, Nir Friedman, and Stuart Russell. Bayesian Q-learning. In *AAAI/IAAI*, pages 761–768, 1998.
- [8] Richard Dearden, Nir Friedman, and David Andre. Model based Bayesian exploration. In *UAI*, pages 150–159, 1999.
- [9] Justin Fu, John D Co-Reyes, and Sergey Levine. EX2: Exploration with exemplar models for deep reinforcement learning. *arXiv preprint arXiv:1703.01260*, 2017.
- [10] Rein Houthoofd, Xi Chen, Yan Duan, John Schulman, Filip De Turck, and Pieter Abbeel. VIME: Variational information maximizing exploration. In *NIPS*, pages 1109–1117, 2016.
- [11] Michael Kearns and Satinder Singh. Near-optimal reinforcement learning in polynomial time. *Mach. Learn.*, 49(2-3):209–232, 2002.
- [12] Diederik Kingma and Jimmy Ba. Adam: A method for stochastic optimization. *arXiv preprint arXiv:1412.6980*, 2014.
- [13] Balaji Lakshminarayanan, Alexander Pritzel, and Charles Blundell. Simple and scalable predictive uncertainty estimation using deep ensembles. *arXiv preprint arXiv:1612.01474*, 2016.

- [14] Volodymyr Mnih, Koray Kavukcuoglu, David Silver, Andrei A Rusu, Joel Veness, Marc G Bellemare, Alex Graves, Martin Riedmiller, Andreas K Fidjeland, Georg Ostrovski, et al. Human-level control through deep reinforcement learning. *Nature*, 518(7540):529–533, 2015.
- [15] Ian Osband and Benjamin Van Roy. Why is posterior sampling better than optimism for reinforcement learning. *arXiv preprint arXiv:1607.00215*, 2016.
- [16] Ian Osband, Dan Russo, and Benjamin Van Roy. (More) efficient reinforcement learning via posterior sampling. In *NIPS*, pages 3003–3011, 2013.
- [17] Ian Osband, Benjamin Van Roy, and Zheng Wen. Generalization and exploration via randomized value functions. *arXiv preprint arXiv:1402.0635*, 2014.
- [18] Ian Osband, Charles Blundell, Alexander Pritzel, and Benjamin Van Roy. Deep exploration via bootstrapped DQN. In *NIPS*, pages 4026–4034, 2016.
- [19] Georg Ostrovski, Marc G Bellemare, Aaron van den Oord, and Remi Munos. Count-based exploration with neural density models. *arXiv preprint arXiv:1703.01310*, 2017.
- [20] Jonathan Sorg, Satinder Singh, and Richard L Lewis. Variance-based rewards for approximate bayesian reinforcement learning. *arXiv preprint arXiv:1203.3518*, 2012.
- [21] Alexander L Strehl, Lihong Li, Eric Wiewiora, John Langford, and Michael L Littman. Pac model-free reinforcement learning. In *ICML*, pages 881–888. ACM, 2006.
- [22] Malcolm Strens. A Bayesian framework for reinforcement learning. In *ICML*, pages 943–950, 2000.
- [23] Yi Sun, Faustino Gomez, and Jürgen Schmidhuber. Planning to be surprised: Optimal Bayesian exploration in dynamic environments. In *ICAGI*, pages 41–51. Springer, 2011.
- [24] Haoran Tang, Rein Houthoofd, Davis Foote, Adam Stooke, Xi Chen, Yan Duan, John Schulman, Filip De Turck, and Pieter Abbeel. # Exploration: A study of count-based exploration for deep reinforcement learning. *arXiv preprint arXiv:1611.04717*, 2016.
- [25] Hado Van Hasselt, Arthur Guez, and David Silver. Deep reinforcement learning with double Q-learning. In *AAAI*, pages 2094–2100, 2016.
- [26] Christopher JCH Watkins and Peter Dayan. Q-learning. *Mach. Learn.*, 8(3-4):279–292, 1992.
- [27] Christopher John Cornish Hellaby Watkins. *Learning from delayed rewards*. PhD thesis, University of Cambridge England, 1989.

A Hyperparameters

We tabulate the hyperparameters in our well-tuned implementation of double DQN in Table 1:

hyperparameter	value	descriptions
total training frames	40 million	Length of training for each game.
minibatch size	32	Size of minibatch samples for each parameter update.
replay buffer size	1000000	The number of most recent frames stored in replay buffer.
agent history length	4	The number of most recent frames concatenated as input to the Q network. Total number of iterations = total training frames / agent history length.
target network update frequency	10000	The frequency of updating target network, in the number of parameter updates.
discount factor	0.99	Discount factor for Q value.
action repeat	4	Repeat each action selected by the agent this many times. A value of 4 means the agent sees every 4th frame.
update frequency	4	The number of actions between successive parameter updates.
optimizer	Adam	Optimizer for parameter updates.
β_1	0.9	Adam optimizer parameter.
β_2	0.99	Adam optimizer parameter.
ϵ	10^{-4}	Adam optimizer parameter.
learning rate schedule	$\begin{cases} 10^{-4} & t \leq 10^6 \\ \text{Interp}(10^{-4}, 5 * 10^{-5}) & \text{otherwise} \\ 5 * 10^{-5} & t > 5 * 10^6 \end{cases}$	Learning rate for Adam optimizer, as a function of iteration t .
exploration schedule	$\begin{cases} \text{Interp}(1, 0.1) & t < 10^6 \\ \text{Interp}(0.1, 0.01) & \text{otherwise} \\ 0.01 & t > 5 * 10^6 \end{cases}$	Probability of random action in ϵ -greedy exploration, as a function of the iteration t .
replay start size	50000	Number of uniform random actions taken before learning starts.

Table 1: Double DQN hyperparameters. These hyperparameters are selected based on performances of seven Atari games: Beam Rider, Breakout, Pong, Enduro, Qbert, Seaquest, and Space Invaders. $\text{Interp}(\cdot, \cdot)$ is linear interpolation between two values.

B Results tables

	Bootstrapped DQN	Double DQN	Ensemble Voting	UCB-Exploration
Alien	1445.1	2059.7	2282.8	2817.6
Amidar	430.58	667.5	683.72	663.8
Assault	2519.06	2820.61	3213.58	3702.76
Asterix	3829.0	7639.5	8740.0	8732.0
Asteroids	1009.5	1002.3	1149.3	1007.8
Atlantis	1314058.0	1982677.0	1786305.0	2016145.0
Bank Heist	795.1	789.9	869.4	906.9
Battle Zone	26230.0	24880.0	27430.0	26770.0
Beam Rider	8006.58	7743.74	7991.9	9188.26
Bowling	28.62	30.92	32.92	38.06
Boxing	85.91	94.07	94.47	98.08
Breakout	400.22	467.45	426.78	411.31
Centipede	5328.77	5177.51	6153.28	6237.18
Chopper Command	2153.0	3260.0	3544.0	3677.0
Crazy Climber	110926.0	124456.0	126677.0	127754.0
Demon Attack	9811.45	23562.55	30004.4	59861.9
Double Dunk	-10.82	-14.58	-11.94	-4.08
Enduro	1314.31	1439.59	1999.88	2752.55
Fishing Derby	21.89	23.69	30.02	29.71
Freeway	33.57	32.93	33.92	33.96
Frostbite	1284.8	529.2	1196.0	1903.0
Gopher	7652.2	12030.0	10993.2	12910.8
Gravitar	227.5	279.5	371.5	318.0
Ice Hockey	-4.62	-4.63	-1.73	-4.71
Jamesbond	594.5	594.0	602.0	710.0
Kangaroo	8186.0	7787.0	8174.0	14196.0
Krull	8537.52	8517.91	8669.17	9171.61
Kung Fu Master	24153.0	32896.0	30988.0	31291.0
Montezuma Revenge	2.0	4.0	1.0	4.0
Ms Pacman	2508.7	2498.1	3039.7	3425.4
Name This Game	8212.4	9806.9	9255.1	9570.5
Pitfall	-5.99	-7.57	-3.37	-1.47
Pong	21.0	20.67	21.0	20.95
Private Eye	1815.19	788.63	1845.28	1252.01
Qbert	10557.25	6529.5	12036.5	14198.25
Riverraid	11528.0	11834.7	12785.8	15622.2
Road Runner	52489.0	49039.0	54768.0	53596.0
Robotank	21.03	29.8	31.83	41.04
Seaquest	9320.7	18056.4	20458.6	24001.6
Space Invaders	1549.9	1917.5	1890.8	2626.55
Star Gunner	20115.0	52283.0	41684.0	47367.0
Tennis	-15.11	-14.04	-11.63	-7.8
Time Pilot	5088.0	5548.0	6153.0	6490.0
Tutankham	167.47	223.43	208.61	200.76
Up N Down	9049.1	11815.3	19528.3	19827.3
Venture	115.0	96.0	78.0	67.0
Video Pinball	364600.85	374686.89	343380.29	372564.11
Wizard Of Wor	2860.0	3877.0	5451.0	5873.0
Zaxxon	592.0	8903.0	3901.0	3695.0
Times best	1	7	9	30

Table 2: Comparison of maximal mean rewards achieved by agents. Maximal mean reward is calculated in a window of 100 consecutive episodes. Bold denotes the highest value in each row.

	Ensemble Voting	UCB-Exploration	A3C+
Alien	2282.8	2817.6	1848.33
Amidar	683.72	663.8	964.77
Assault	3213.58	3702.76	2607.28
Asterix	8740.0	8732.0	7262.77
Asteroids	1149.3	1007.8	2257.92
Atlantis	1786305.0	2016145.0	1733528.71
Bank Heist	869.4	906.9	991.96
Battle Zone	27430.0	26770.0	7428.99
Beam Rider	7991.9	9188.26	5992.08
Bowling	32.92	38.06	68.72
Boxing	94.47	98.08	13.82
Breakout	426.78	411.31	323.21
Centipede	6153.28	6237.18	5338.24
Chopper Command	3544.0	3677.0	5388.22
Crazy Climber	126677.0	127754.0	104083.51
Demon Attack	30004.4	59861.9	19589.95
Double Dunk	-11.94	-4.08	-8.88
Enduro	1999.88	2752.55	749.11
Fishing Derby	30.02	29.71	29.46
Freeway	33.92	33.96	27.33
Frostbite	1196.0	1903.0	506.61
Gopher	10993.2	12910.8	5948.40
Gravitar	371.5	318.0	246.02
Ice Hockey	-1.73	-4.71	-7.05
Jamesbond	602.0	710.0	1024.16
Kangaroo	8174.0	14196.0	5475.73
Krull	8669.17	9171.61	7587.58
Kung Fu Master	30988.0	31291.0	26593.67
Montezuma Revenge	1.0	4.0	142.50
Ms Pacman	3039.7	3425.4	2380.58
Name This Game	9255.1	9570.5	6427.51
Pitfall	-3.37	-1.47	-155.97
Pong	21.0	20.95	17.33
Private Eye	1845.28	1252.01	100.0
Qbert	12036.5	14198.25	15804.72
Riverraid	12785.8	15622.2	10331.56
Road Runner	54768.0	53596.0	49029.74
Robotank	31.83	41.04	6.68
Seaquest	20458.6	24001.6	2274.06
Space Invaders	1890.8	2626.55	1466.01
Star Gunner	41684.0	47367.0	52466.84
Tennis	-11.63	-7.8	-20.49
Time Pilot	6153.0	6490.0	3816.38
Tutankham	208.61	200.76	132.67
Up N Down	19528.3	19827.3	8705.64
Venture	78.0	67.0	0.00
Video Pinball	343380.29	372564.11	35515.92
Wizard Of Wor	5451.0	5873.0	3657.65
Zaxxon	3901.0	3695.0	7956.05
Times Best	10	28	10

Table 3: Comparison of Ensemble Voting, UCB Exploration, both trained with 40 million frames and A3C+ of [3], trained with 200 million frames

Category	Total	Bootstrapped DQN	Double DQN	Ensemble Voting	UCB-Exploration
Human Optimal	23	0	3	5	15
Score Explicit	8	0	2	1	5
Dense Reward	8	0	1	1	6
Sparse Reward	5	1	0	2	2

Table 4: Comparison of each method across different game categories. The Atari games are separated into four categories: human optimal, score explicit, dense reward, and sparse reward. In each row, we present the number of games in this category, the total number of games where each algorithm achieves the optimal performance according to Table 2. The game categories follow the taxonomy in Table 1 of [19]

C InfoGain exploration

In this section, we also studied an ‘‘InfoGain’’ exploration bonus, which encourages agents to gain information about the Q^* -function and examine its effectiveness. We found it had some benefits on top of Ensemble Voting, but no uniform additional benefits once already using Q-ensembles on top of Double DQN. We describe the approach and our experimental findings here.

Similar to Sun et al. [23], we define the information gain from observing an additional transition τ_n as

$$H_{\tau_t|\tau_1,\dots,\tau_{n-1}} = D_{KL}(\tilde{p}(Q^*|\tau_1,\dots,\tau_n)||\tilde{p}(Q^*|\tau_1,\dots,\tau_{n-1}))$$

where $\tilde{p}(Q^*|\tau_1,\dots,\tau_n)$ is the posterior distribution of Q^* after observing a sequence of transitions (τ_1,\dots,τ_n) . The total information gain is

$$H_{\tau_1,\dots,\tau_N} = \sum_{n=1}^N H_{\tau_n|\tau_1,\dots,\tau_{n-1}}. \quad (14)$$

Our Ensemble Voting, Algorithm 1, does not maintain the posterior \tilde{p} , thus we cannot calculate (14) explicitly. Instead, inspired by Lakshminarayanan et al. [13], we define an InfoGain exploration bonus that measures the disagreement among $\{Q_k\}$. Note that

$$H_{\tau_1,\dots,\tau_N} + H(\tilde{p}(Q^*|\tau_1,\dots,\tau_N)) = H(p(Q^*)),$$

where $H(\cdot)$ is the entropy. If H_{τ_1,\dots,τ_N} is small, then the posterior distribution has high entropy and high residual information. Since $\{Q_k\}$ are approximate samples from the posterior, high entropy of the posterior leads to large discrepancy among $\{Q_k\}$. Thus, the exploration bonus is monotonous with respect to the residual information in the posterior $H(\tilde{p}(Q^*|\tau_1,\dots,\tau_N))$. We first compute the Boltzmann distribution for each Q_k

$$P_{\mathbb{T},k}(a|s) = \frac{\exp(Q_k(s,a)/\mathbb{T})}{\sum_{a'} \exp(Q_k(s,a')/\mathbb{T})},$$

where $\mathbb{T} > 0$ is a temperature parameter. Next, calculate the average Boltzmann distribution

$$P_{\mathbb{T},\text{avg}} = \frac{1}{K} \cdot \sum_{k=1}^K P_{\mathbb{T},k}(a|s).$$

The InfoGain exploration bonus is the average KL-divergence from $\{P_{\mathbb{T},k}\}_{k=1}^K$ to $P_{\mathbb{T},\text{avg}}$

$$b_{\mathbb{T}}(s) = \frac{1}{K} \cdot \sum_{k=1}^K D_{KL}[P_{\mathbb{T},k}||P_{\mathbb{T},\text{avg}}]. \quad (15)$$

The modified reward is

$$\hat{r}(s,a,s') = r(s,a) + \rho \cdot b_{\mathbb{T}}(s), \quad (16)$$

where $\rho \in \mathbb{R}_+$ is a hyperparameter that controls the degree of exploration.

The exploration bonus $b_{\mathbb{T}}(s_t)$ encourages the agent to explore where $\{Q_k\}$ disagree. The temperature parameter \mathbb{T} controls the sensitivity to discrepancies among $\{Q_k\}$. When $\mathbb{T} \rightarrow +\infty$, $\{P_{\mathbb{T},k}\}$ converge to the uniform distribution on the action space and $b_{\mathbb{T}}(s) \rightarrow 0$. When \mathbb{T} is small, the differences among $\{Q_k\}$ are magnified and $b_{\mathbb{T}}(s)$ is large.

We display Algorithm 3, which incorporates our InfoGain exploration bonus into Algorithm 2. The hyperparameters λ , \mathbb{T} and ρ vary for each game.

Algorithm 3 UCB + InfoGain Exploration with Q -Ensembles

- 1: **Input:** Value function networks Q with K outputs $\{Q_k\}_{k=1}^K$. Hyperparameters T , λ , and ρ .
 - 2: Let B be a replay buffer storing experience for training.
 - 3: **for** each episode **do**
 - 4: Obtain initial state from environment s_0
 - 5: **for** step $t = 1, \dots$ until end of episode **do**
 - 6: Pick an action according to $a_t \in \operatorname{argmax}_a \{\tilde{\mu}(s_t, a) + \lambda \cdot \tilde{\sigma}(s_t, a)\}$
 - 7: Receive state s_{t+1} and reward r_t from environment, having taken action a_t
 - 8: Calculate exploration bonus $b_T(s_t)$ according to (15)
 - 9: Add $(s_t, a_t, r_t + \rho \cdot b_T(s_t), s_{t+1})$ to replay buffer B
 - 10: At learning interval, sample random minibatch and update $\{Q_k\}$
 - 11: **end for**
 - 12: **end for**
-

C.1 Performance of UCB+InfoGain exploration

We demonstrate the performance of the combined UCB+InfoGain exploration in Figure 3 and Figure 3. We augment the previous figures in Section 5 with the performance of ucb+infogain exploration, where we set $\lambda = 0.1$, $\rho = 1$, and $T = 1$ in Algorithm 3.

Figure 3 shows that combining UCB and InfoGain exploration does not lead to uniform improvement in the normalized learning curve.

At the individual game level, Figure 3 shows that the impact of InfoGain exploration varies. UCB exploration achieves sufficient exploration in games including Demon Attack and Kangaroo and Riverraid, while InfoGain exploration further improves learning on Enduro, Seaquest, and Up N Down. The effect of InfoGain exploration depends on the choice of the temperature T . The optimal temperature parameter varies across games. In Figure 5, we display the behavior of ucb+infogain exploration with different temperature values. Thus, we see the InfoGain exploration bonus, tuned with the appropriate temperature parameter, can lead to improved learning for games that require extra exploration, such as ChopperCommand, KungFuMaster, Seaquest, UpNDown.

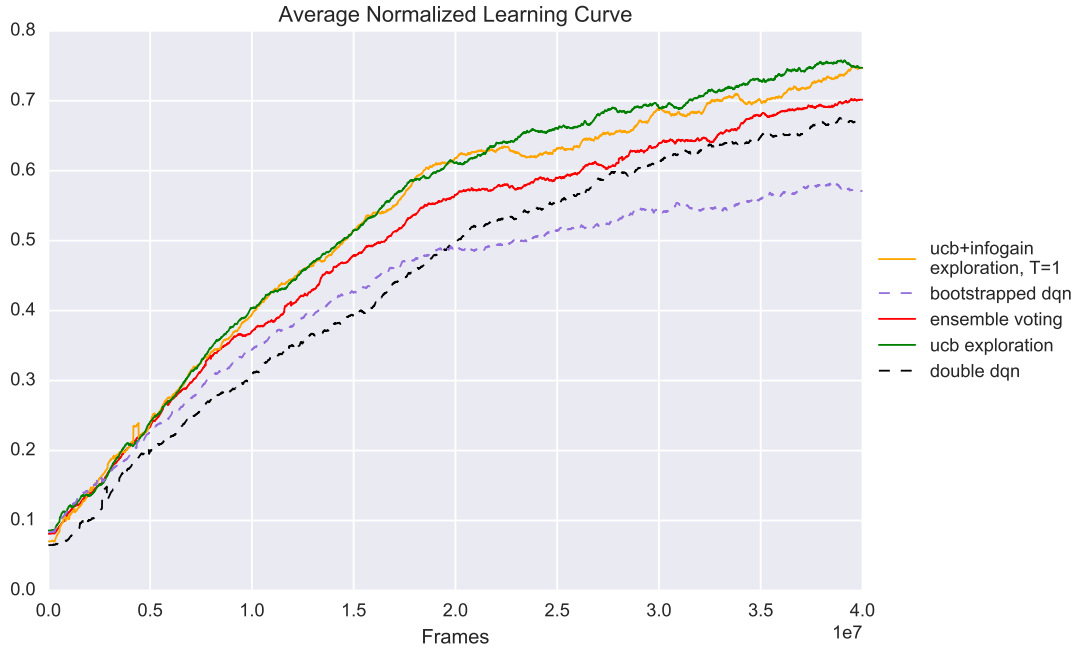


Figure 3: Comparison of all algorithms in normalized curve. The normalized learning curve is calculated as follows: first, we normalize learning curves for all algorithms in the same game to the interval $[0, 1]$; next, average the normalized learning curve from all games for each algorithm.

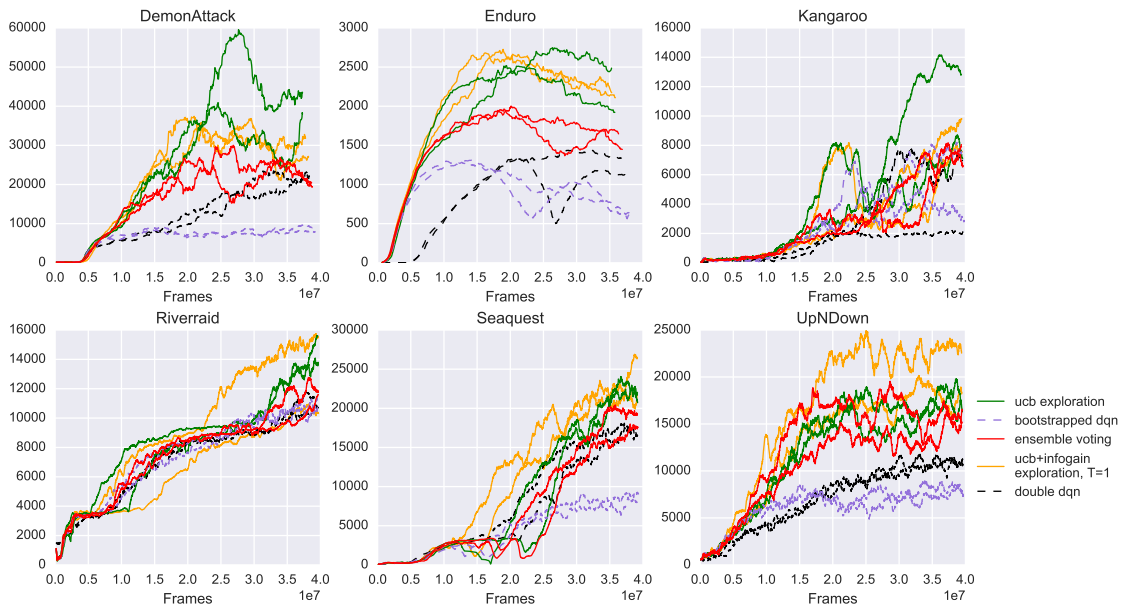


Figure 4: Comparison of algorithms against Double DQN and bootstrapped DQN.

C.2 UCB+InfoGain exploration with different temperatures

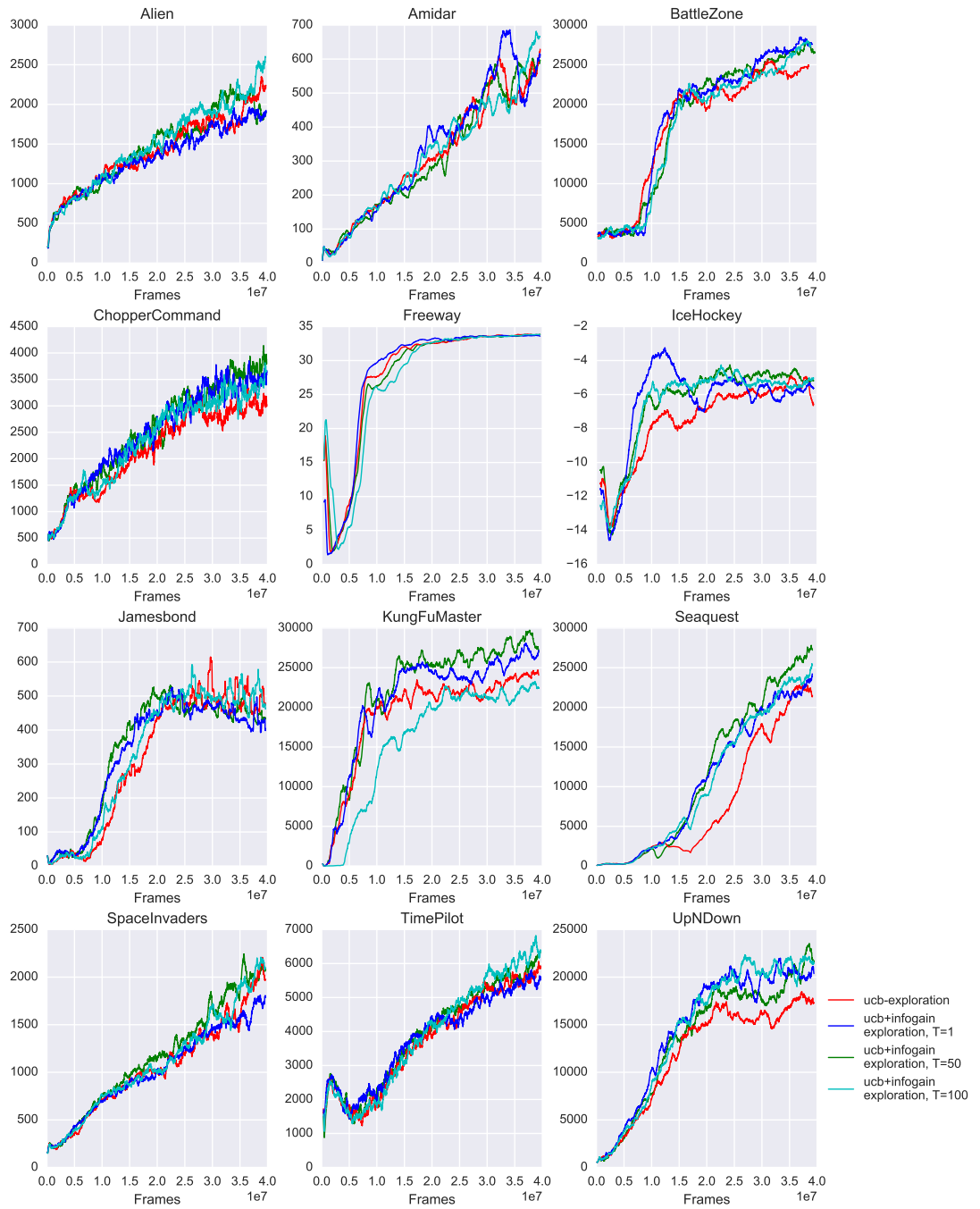


Figure 5: Comparison of UCB+InfoGain exploration with different temperatures versus UCB exploration.